THz quantum cascade lasers with wafer bonded active regions

M. Brandstetter,[1,*] C. Deutsch,[1] A. Benz,[1] G. D. Cole,[2] H. Detz,[3] A. M. Andrews,[3] W. Schrenk,[3] G. Strasser,[3] and K. Unterrainer[1]

[1] *Photonics Institute and Center for Micro- and Nanostructures, Vienna University of Technology, Gusshausstrasse 29, A-1040 Vienna, Austria*
[2] *Vienna Center for Quantum Science and Technology (VCQ), Faculty of Physics, University of Vienna, Boltzmanngasse 5, A-1090 Vienna, Austria*
[3] *Institute of Solid-State Electronics and Center for Micro- and Nanostructures, Vienna University of Technology, Floragasse 7, A-1040 Vienna, Austria*

[*] *martin.brandstetter@tuwien.ac.at*

Abstract: We demonstrate terahertz quantum-cascade lasers with a 30 μm thick double-metal waveguide, which are fabricated by stacking two 15 μm thick active regions using a wafer bonding process. By increasing the active region thickness more optical power is generated inside the cavity, the waveguide losses are decreased and the far-field is improved due to a larger facet aperture. In this way the output power is increased by significantly more than a factor of 2 without reducing the maximum operating temperature and without increasing the threshold current.

© 2012 Optical Society of America

OCIS codes: (140.5965) Semiconductor lasers, quantum cascade; (140.3070) Infrared and far-infrared lasers.

References and links

1. R. Koehler, A. Tredicucci, F. Beltram, H. E. Beere, E. H. Linfield, A. G. Davies, D. A. Ritchie, R. C. Iotti, and F. Rossi, "Terahertz semiconductor-heterostructure laser," Nature **417**, 156–159 (2002).
2. M. Tonouchi, "Cutting-edge terahertz technology," Nat. Photonics **1**, 97–105 (2007).
3. S. Fathololoumi, E. Dupont, C. Chan, Z. Wasilewski, S. Laframboise, D. Ban, A. Mtys, C. Jirauschek, Q. Hu, and H. C. Liu, "Terahertz quantum cascade lasers operating up to 200 K with optimized oscillator strength and improved injection tunneling," Opt. Express **20**, 3866–3876 (2012).
4. M. Fischer, G. Scalari, K. Celebi, M. Amanti, C. Walther, M. Beck, and J. Faist, "Scattering processes in terahertz InGaAs/InAlAs quantum cascade lasers," Appl. Phys. Lett. **97**, 221114 (2010).
5. C. Deutsch, A. Benz, H. Detz, P. Klang, M. Nobile, A. M. Andrews, W. Schrenk, T. Kubis, P. Vogl, G. Strasser, and K. Unterrainer, "Terahertz quantum cascade lasers based on type II InGaAs/GaAsSb/InP," Appl. Phys. Lett. **97**, 1110 (2010).
6. K. Unterrainer, R. Colombelli, C. Gmachl, F. Capasso, H. Y. Hwang, A. M. Sergent, D. L. Sivco, and A. Y. Cho, "Quantum cascade lasers with double metal-semiconductor waveguide resonators," Appl. Phys. Lett. **80**, 3060–3062 (2002).
7. G. Fasching, V. Tamošiūnas, A. Benz, A. M. Andrews, K. Unterrainer, R. Zobl, T. Roch, W. Schrenk, and G. Strasser, "Subwavelength microdisk and microring terahertz quantum-cascade lasers," IEEE J. Quantum Electron. **43**, 687–697 (2007).
8. A. Benz, C. Deutsch, G. Fasching, K. Unterrainer, A. M. Andrews, P. Klang, W. Schrenk, and G. Strasser, "Active photonic crystal terahertz laser," Opt. Express **17**, 941–946 (2009).
9. B. Williams, S. Kumar, Q. Hu, and J. Reno, "High-power terahertz quantum-cascade lasers," Electron. Lett. **42**, 89 (2006).
10. M. I. Amanti, M. Fischer, G. Scalari, M. Beck, and J. Faist, "Low-divergence single-mode terahertz quantum cascade laser," Nat. Photonics **3**, 586–590 (2009).
11. L. Mahler, A. Tredicucci, F. Beltram, C. Walther, J. Faist, B. Witzigmann, H. E. Beere, and D. A. Ritchie, "Vertically emitting microdisk lasers," Nat. Photonics **3**, 46–49 (2009).

#171346 - $15.00 USD Received 27 Jun 2012; revised 17 Aug 2012; accepted 23 Aug 2012; published 2 Oct 2012

12. Y. Chassagneux, R. Colombelli, W. Maineult, S. Barbieri, H. E. Beere, D. A. Ritchie, S. P. Khanna, E. H. Linfield, and A. G. Davies, "Electrically pumped photonic-crystal terahertz lasers controlled by boundary conditions," Nature **457**, 174–178 (2009).
13. Y. Okuno, K. Uomi, M. Aoki, and T. Tsuchiya, "Direct wafer bonding of IIIV compound semiconductors for free-material and free-orientation integration," IEEE J. Quantum Electron. **33**, 959–969 (1997).
14. A. Black, A. R. Hawkins, N. M. Margalit, D. I. Babic, A. L. Holmes, Jr., Y.-L. Chang, P. Abraham, J. E. Bowers, and E. L. Hu, "Wafer fusion: Materials issues and device results," IEEE J. Sel. Top. Quantum Electron. **3**, 943–951 (1997).
15. M. A. Ordal, L. L. Long, R. J. Bell, S. E. Bell, R. R. Bell, R. W. Alexander, Jr., and C. A. Ward, "Optical properties of the metals Al, Co, Cu, Au, Fe, Pb, Ni, Pd, Pt, Ag, Ti, and W in the infrared and far infrared," Appl. Opt. **22**, 1100–1120 (1983).
16. "Comsol multiphysics, http://www.comsol.com," .
17. S. Kohen, B. S. Williams, and Q. Hu, "Electromagnetic modeling of terahertz quantum cascade laser waveguides and resonators," J. Appl. Phys. **97**, 053106 (2005).
18. B. S. Williams, H. Callebaut, S. Kumar, Q. Hu, and J. L. Reno, "3.4 THz quantum cascade laser based on longintudinal-optical-phonon scattering for depopulation," Appl. Phys. Lett. **82**, 1015–1017 (2003).

1. Introduction

Since their first demonstration in 2001 [1] much effort has been put into increasing the performance of terahertz (THz) quantum cascade lasers (QCLs). Due to their small size and high output power, these devices are very attractive for multiple applications in the THz spectral region, for example in the field of industrial material inspection, security, biological or medical sciences and for information and communication technology [2]. One of the main challenges is to improve the temperature performance in order to reach a regime where thermoelectric cooling is possible. One approach is by optimizing the active region. The maximum operating temperature of 199.5 K [3] is achieved using an optimized 3 well resonant phonon design, where the lower laser level is depopulated via the inelastic emission of a longitudinal optical (LO) phonon. Another promising alternative involves switching from the commonly used GaAs/AlGaAs material system to one with lower effective mass, in order to achieve higher optical gain. THz QCLs in the InGaAs/InAlAs [4] or InGaAs/GaAsSb [5] material systems were demonstrated previously. So far GaAs/AlGaAs THz QCLs still outperform devices based on other material systems.

Besides the active region, the waveguide is very important for the performance of THz QCLs. The highest operating temperature is achieved by using double-metal (DM) waveguides [6], where the light is guided in the active region between 2 metal layers. Using this concept various resonator types can be fabricated for example ridges, disks [7] or photonic crystals [8]. One drawback of this concept is that the light is quenched in a sub-wavelength structure, which leads to a large mismatch of the cavity mode to the free space mode. Thus the reflectivity is increased, but on the other hand the outcoupled power is decreased. The highest output power is achieved with a single plasmon waveguide, where the light is confined between a top metal layer and a highly doped layer on the bottom. The confinement of the mode is weaker at the bottom thus it leaks into the substrate. This leads to a better match with the free space mode and thus to a lower facet reflectivity. With this concept, output powers of up to 248 mW in pulsed mode are achieved [9]. However, one disadvantage is the lower confinement factor when compared to DM waveguides, increasing the threshold current and thus reducing the temperature performance. Other approaches to tailor the outcoupled power and to improve the far-field are by using third order DFB structures [10], surface emitting DFB ring resonators [11] or photonic crystal resonators [12] which can be implemented in a DM waveguide geometry. These concepts require the approprite design of the resonator.

An increased active region thickness decreases the waveguide losses, improves the matching of the guided cavity- and the free space mode and increases the generated light in the cavity. Since the growth of thick structures by molecular beam epitaxy (MBE) would take unreason-

#171346 - $15.00 USD Received 27 Jun 2012; revised 17 Aug 2012; accepted 23 Aug 2012; published 2 Oct 2012
(C) 2012 OSA

ably long time, we use a wafer bonding step to directly bond 2 active region samples together without any intermediate layer. This concept has already been employed for combining different semiconductor material systems [13] [14]. We utilize a DM waveguide in order to obtain a high confinement of the optical mode. We show that the collected output power is increased by significantly more than a factor of 2 when compared to a device with single active region, without affecting the temperature performance. Furthermore the far-field is improved due to the larger aperture of the laser facet without the need to design an elaborate DFB or photonic crystal structure.

2. THz QCLs with increased waveguide thickness

We calculate the waveguide losses and intensity distribution of a double-metal waveguide using a one dimensional waveguide solver. We assume an emission frequency of 4.2 THz, which has been obtained from measurements. The active region is assumed to be lossless, while the gold layers are modelled using Drude parameters [15]. Figure 1(a) shows the calculated intensity of the TEM mode in the active region between the two gold waveguide layers for a 15 μm thick active region (red solid line). The dashed black line indicates the absolute value of the refractive index of the respective material. For the 30 μm thick wafer bonded THz QCL, the highly doped top and bottom contact layers at the bonding interface are not removed. Therefore a 165 nm thick n+ doped layer is located between the bonded samples, leading to a drop in the intensity, which can be seen in Fig. 1(b). The calculations show that increasing the thickness of a DM waveguide from 15 μm to 30 μm leads to a reduction of the waveguide losses by nearly a factor of 2. The highly doped n+ GaAs layer between the bonded active regions as well as the top and bottom contact layers have a neglectable influence on the total waveguide losses.

We investigate the influence of the waveguide thickness on the reflectivity using a commercial finite element solver [16]. We make use of a 2-dimensional model, assuming a bottom contact layer, which extends beyond the laser facet, modelling a device with facets defined by reactive ion etching (RIE). In Fig. 1(c) the reflectivity of a DM waveguide is plotted versus the active region thickness for a frequency of 4.2 THz. The blue dotted lines indicate the values for the experimentally investigated active region thicknesses. The reflectivity shows a minimum at 20 μm and oscillates with increasing waveguide thickness. This can be attributed to resonant effects, which have been already described theoretically [17].

It can be seen that at an emission frequency of 4.2 THz the reflectivity of a 15 μm and a 30 μm thick waveguide is almost equal. Therefore we have chosen an active region emitting at this frequency, allowing us to neglect the influence of the reflectivity on the experimentally obtained output power and temperature performance.

3. Fabrication

The active region is based on a 4-well resonant phonon depletion design [18] which has been grown via MBE in the GaAs/$Al_{0.15}Ga_{0.85}As$ material system on a GaAs substrate. The structure is repeated 271 times giving a total thickness of 15 μm . The designed emission frequency is 4.2 THz. In order to improve the contact resistance n+ doped GaAs contact layers have been grown on top and bottom of the active region with 60 nm and a 100 nm thickness respectively with an additional 5 nm thick n+ doped $In_{50}Ga_{50}As$ layer on the top contact. We coat the active region with gold in order to attach it with the epitaxial side down to a carrier substrate via a gold-gold thermo-compression bonding process using a commercial wafer bonding system (EVG 501). Then the substrate is removed by a polishing/ etching step. After thorough surface cleaning and oxide removal a second piece of the wafer with the epitaxially grown active region is bonded directly on top of the first one by direct wafer bonding using the same system (EVG 501) as in the thermo-compression bonding step. We apply a pressure of 2 MPa at a

#171346 - $15.00 USD Received 27 Jun 2012; revised 17 Aug 2012; accepted 23 Aug 2012; published 2 Oct 2012
(C) 2012 OSA

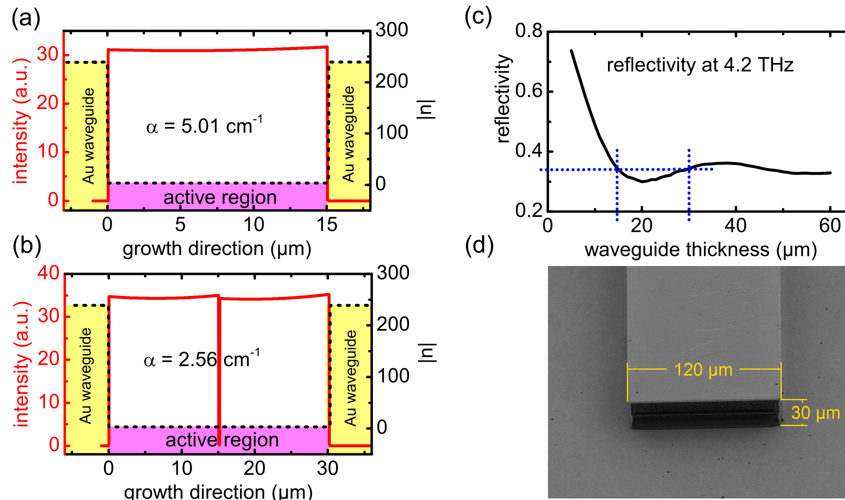

Fig. 1. Calculated intensity inside the waveguide for (a) 15 μm and (b) 30 μm active region thickness (red solid line). The black dashed line indicates the refractive index of the respective material. (c) Reflectivity of a double-metal waveguide with etched facet at varying thickness. For the experiment the emitting frequency is chosen such that the reflectivity at 15 μm and 30 μm is almost equal. (d) SEM picture of a fabricated device.

temperature of 420 °C. For this step no additional adhesion or metal layer is used in between the two samples. The active regions are both stacked with the epitaxial side down in order to be operated in the same direction. In this way we fabricate a 30 μm thick active region. After substrate removal ridge resonators are defined from the material using RIE, where the top gold layer of the DM waveguide acts as etch mask. We employ etched facets where the bottom contact layer extends over the edges of the device. Figure 1(d) shows a SEM picture of a wafer bonded THz QCL with a width of 120 μm . The wafer bonding interface can be clearly seen because of slight under etching of the top active region due to the RIE process.

4. Experimental results and discussion

The fabricated devices are mounted in a liquid helium flow cryostat which is attached to a FTIR spectrometer. The temperature dependent integral measurements and spectral characteristics are recorded using a pyroelectric (DTGS) detector. The peak values of the power in the measured voltage- light vs. current density (VLI) plots are adjusted to the absolute power measured using a calibrated thermopile detector, mounted inside the cryostat in close vicinity (2 mm) to the devices. The output power values are uncorrected regarding the collection efficiency. In Fig. 2 the measured VLI plots at different temperatures for a device with (a) 15 μm and (b) 30 μm active region thickness are depicted. The QCLs are operated in pulsed mode with 200 ns pulse duration and 10 kHz repetition frequency, gated with 10 Hz.

The measurements show that the maximum operating temperature is comparable for both active region thicknesses, which can be attributed to the low threshold current of the active region, leading to low heat dissipation inside the cavity. The threshold current densities are comparable as well.

The threshold voltage is twice as high for a 30 μm thick device compared to a 15 μm device. This indicates an excellent electrical interface quality in terms of a low contact voltage between the bonded active regions.

#171346 - $15.00 USD Received 27 Jun 2012; revised 17 Aug 2012; accepted 23 Aug 2012; published 2 Oct 2012
(C) 2012 OSA

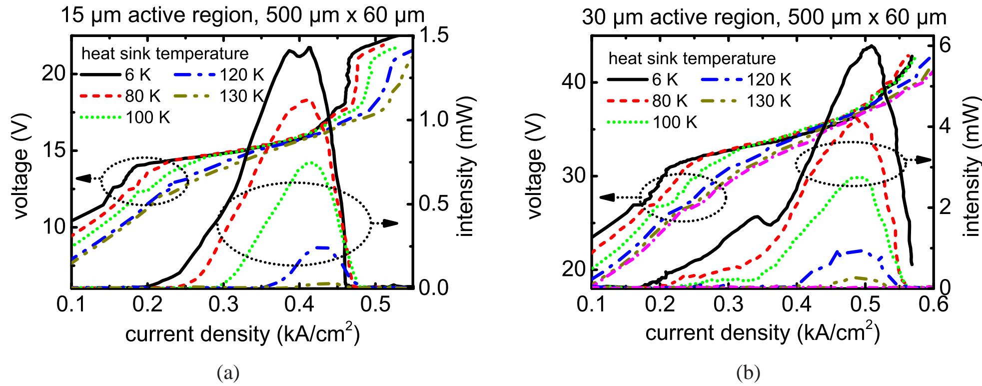

Fig. 2. Temperature characteristics of a device with (a) 15 μm and (b) 30 μm active region. The threshold current densities and maximum operating temperature are comparable for both devices. The threshold voltage for a 30 μm device is increased by a factor of 2 compared to the single active region device, indicating a good electrical interface quality in terms of the contact voltage.

In Table 1 the maximum measured output power for devices with different dimensions is shown. The devices are operated at a temperature of 6 K heat sink temperature in pulsed mode with 200 ns pulse duration and 200 kHz repetition frequency. The measured output power of the wafer bonded devices is significantly more than 2 times higher compared to devices with single active region. Thus by doubling the electrical input power, the optical output power is increased by a factor larger than 2. This is in part due to the doubled active material, producing twice as much optical gain inside the cavity. Furthermore the waveguide losses are reduced for waveguides with increased thickness and the far-field is improved due to the larger facet aperture, leading to a better collection efficiency at the detector. The maximum measured output powers are 5 mW for a 15 μm device and 17 mW for a 30 μm device.

	Active region thickness (μm)	
Device dimension (μm)	**15**	**30**
1000 x 120	5 mW	13 mW
1000 x 60	2.5 mW	17 mW
500 x 120	2 mW	7 mW
500 x 60	1.4 mW	6 mW

Table 1. Maximum output power of devices with different dimensions and 15 μm and 30 μm active region thickness respectively. The maximum value of a 30 μm thick device is larger by significantly more than a factor of 2 compared to a single active region device.

We have measured the far-field of 15 μm and 30 μm thick devices using a pyroelectric detector, which is mounted on a 2-dimensional translation stage. The detector is placed in front of the TPX cryostat window at a distance of 6.5 cm to the laser facet. The QCL is operated at the bias voltage corresponding to the maximum output power in pulsed mode with 2 μs pulse duration and 100 kHz repetition frequency, gated with 25 Hz. The measured data are transformed into angular coordinates. The measured intensities are corrected for the projection on a sphere. Figure 3 shows the measured far-field pattern for a device with (a) 15 μm and (b) 30 μm active region thickness. The resonators are of similar dimensions and both devices show

#171346 - $15.00 USD   Received 27 Jun 2012; revised 17 Aug 2012; accepted 23 Aug 2012; published 2 Oct 2012
(C) 2012 OSA

single mode emission at 4.2 THz.

It can be seen that the fringes, originating from the interference with the emission from the back facet, are much less pronounced for the device with 30 μm waveguide thickness. This reduced fringe visibility is attributed to a better collimated output beam due to the larger facet aperture. The maximum of the emission intensity is at an angle of $\vartheta = 15^{\circ}$, which is due to the reflection at the extended gold bottom contact layer. In the lower part of Fig. 3 (a) and (b) the cross section of the measured far-field plots in the symmetry plane (indicated by the dashed line) is compared to a 2-dimensional simulation, which is performed using a commercial finite element solver [16]. The simulation matches the measured data and confirms the improved far-field in terms of a reduced interference pattern.

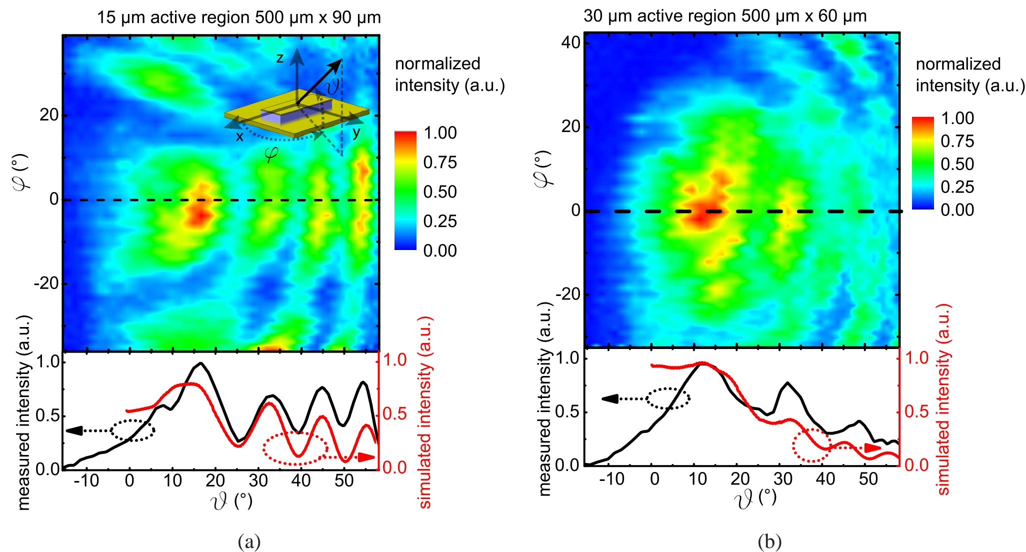

Fig. 3. Experimentally measured far-field of a device with (a) 15 μm and (b) 30 μm active region. The lower plots show the intensity along the dashed line, which is compared to a 2-dimensional finite-element simulation. The far-field is improved significantly for the thick device in terms of a reduced fringe visibility and a better collimated beam, which is also confirmed by the simulation.

5. Conclusion

We have fabricated THz QCLs with a 30 μm thick DM waveguide by direct wafer bonding of two identical 15 μm thick active regions. Calculations show that the waveguide losses are reduced by increasing the waveguide thickness. The threshold current density and operating temperature of 30 μm thick devices are comparable to the values of single active region devices. The threshold voltage is only increased by a factor of 2 indicating an excellent bonding interface with negligible contact resistance. The measured output power is increased by more than a factor of 2, which can be attributed to the lower waveguide losses and the improved far-field due to the increased facet aperture. In this way high power THz QCLs can be fabricated from stacked active regions with commonly used thickness, without the drawback of lower maximum operating temperature and increased threshold current of surface plasmon waveguides.

The authors acknowledge financial support by the Austrian Scientific Fund FWF (SFB-IRON F2511, and DK CoQuS W1210), the Austrian Nano Initiative project (PLATON) and the Vienna Science and Technology Fund (WWTF).

#171346 - $15.00 USD Received 27 Jun 2012; revised 17 Aug 2012; accepted 23 Aug 2012; published 2 Oct 2012
(C) 2012 OSA